Astron. Astrophys. 327, 342–348 (1997)

ASTRONOMY AND ASTROPHYSICS

High mass-loss carbon stars and the evolution of the local $^{12}C/^{13}C$ ratio

J.S. Greaves and W.S. Holland

Joint Astronomy Centre, 660 N. A'ōhōku Place, University Park, Hilo, Hawaii 96720, USA

Received 11 February 1997 / Accepted 12 June 1997

Abstract. The $^{12}C/^{13}C$ ratio has been measured in a sample of 10 carbon stars with high mass-loss rates, of $\geq 10^{-5}$ $M_\odot$ yr^{-1}. This sample is complete for northern hemisphere carbon stars within $\sim$ 1 kpc of the Sun. Using the J=2–1 rotational lines of CO and ^{13}CO, the intensity ratio of $^{12}CO/^{13}CO$ is found to be 17 $\pm$ 11 for the sample, and the deduced $^{12}C/^{13}C$ abundance ratio, after corrections for CO optical depth effects, is 25 $\pm$ 13. The isotopic ratios are rather uniform (12–36 for 9 of the 10 stars), and there are no stars with very low $^{12}C/^{13}C$ values, such as the ratios of 3–4 found for a few low mass-loss carbon stars.

The ejecta from the high mass-loss objects will dominate the evolution of the $^{12}C/^{13}C$ ratio in the local interstellar medium, since mass return is dominated by AGB stars, and the stars of the highest $\dot{M}$ return the majority of the carbon. Thus the ejection of ^{13}C-rich material from AGB stars could explain the evolution of the local $^{12}C/^{13}C$ ratio from 89 at the time of the Sun's formation, to 60–70 now. From our data, it is estimated that the local ISM ratio should have evolved to $\approx 72 \pm 8$ at the present time, which agrees with ISM observations. The AGB stars can therefore fully explain the enrichment of the local ISM in ^{13}C.

Key words: ISM: abundances – ISM: clouds

1. Introduction

The measurement of element abundances in the interstellar medium (ISM) can trace the past star formation history of the Galaxy. All elements heavier than lithium can only be produced in stellar nucleosynthesis, and the ISM is enriched in these elements when material is ejected from stars. Thus, measuring metal abundances indicates what types of stars, and how many, were present in the past. In particular, the ratios of different isotopes of one element are useful. For example, ^{12}C is produced directly by the triple-alpha process, while ^{13}C is mainly produced from ^{12}C in hydrogen-burning envelopes, thus ^{12}C is a 'primary' product and ^{13}C a 'secondary' one. Since ^{12}C is destroyed to produce ^{13}C in the CNO cycle, processing through successive generations of stars results in a decreasing global $^{12}C/^{13}C$ ratio (e.g. Wilson & Matteucci 1992). Thus measuring the $^{12}C/^{13}C$ ratio traces the past star formation rate and stellar mass function. Detailed modelling of evolving isotope ratios has been done by Prantzos et al. (1996), and using recent values for stellar yields of the various isotopes, they were able to match many observations of ISM isotopic ratios.

The question addressed in this paper is the evolution of the $^{12}C/^{13}C$ ratio in the solar neighbourhood. It is well known that this ratio has decreased since the formation of the Sun, from the solar value of 89 to a current value of $\approx$ 60–70 (Langer & Penzias 1993; Wilson & Matteucci 1992). Qualitatively, this is attributed to enrichment of the ISM in ^{13}C from stellar ejecta, the major sources of which are asymptotic giant branch (AGB) stars, novae, supernovae, and winds from massive stars (Jura 1987). However, *quantitative* estimates of the expected change in $^{12}C/^{13}C$ are lacking, partly due to incomplete knowledge of the $^{12}C/^{13}C$ ratios in the stellar sources. The nucleosynthesis models for these stars are subject to several uncertainties (see Prantzos et al. 1996 for a discussion), so a better approach is to directly measure the isotope ratios in stellar ejecta.

To predict the current value of $^{12}C/^{13}C$ in the solar neighbourhood, we chose to make an accurate estimate of the mean isotope ratio in the *dominant* source of stellar ejecta. Mass return is dominated by AGB stars and planetary nebulae (Jura 1987), for which the total mass-loss rate has been estimated at 3×10^{-10} $M_\odot$ pc^{-2} yr^{-1} in the solar neighbourhood (Jura & Kleinmann 1989, hereafter JK). The next most important mass-losing objects are probably Wolf-Rayet stars, which contribute only $\approx 0.6 \times 10^{-10}$ $M_\odot$ pc^{-2} yr^{-1} (Jura & Kleinmann 1990). We have therefore observed a sample of AGB stars, and further selected only those with C/O ratios > 1, which constitute about half of the high mass-loss AGBs (JK). These carbon-rich stars typically have CO/H_2 abundances of $\approx 10^{-3}$, compared to only $(2-5) \times 10^{-4}$ in oxygen-rich AGBs (Kahane & Jura 1994, Zuckerman & Dyck 1986), so the carbon stars dominate the return of C-isotopes to the ISM.

The source sample is taken from that of JK, who used data from the IRAS database and the Two Micron Sky Survey (TMSS, Neugebauer & Leighton 1969) to compile a catalogue

Send offprint requests to: J.S. Greaves

Table 1. Properties of the sample of high-mass loss stars, selected from the survey by Jura & Kleinmann (1989). The stars are listed in RA order, by IRAS names, together with other names, and identifications from the IRC and CRL catalogues. (For brevity, the IRC or CRL names are used in the next tables.) The types given are C for carbon star, PN for planetary nebula, or PPN for proto-planetary nebula. Distances and mass-loss rates are from Jura & Kleinmann (1989), based on infrared data, and an assumed stellar luminosity of 10^4 $L_\odot$. The estimated CO diameters at half-intensity are deconvolved sizes from our five-point observations (see text), with estimated errors of $\sim \pm 3''$. For IRC+10216 and CRL2688, the diameters are from Truong-Bach et al. (1990, 1991).

IRAS name	other names	type	distance (pc)	$\dot{M}$ (10^{-5} $M_\odot$ yr^{-1})	observed FWHM diameter ($''$)	(10^{17} cm)
06176-1036	CRL915, Red Rectangle	PN	(1100)	(2.3)	—	—
09116-2439	CRL5254	C	1000	1.2	13	1.9
09452+1330	IRC+10216, CRL1381, CW Leo	C	130	1.6	16	0.3
17049-2440	CRL1922	C	960	2.1	28	4.1
18194-2708	CRL2135	C	1000	1.1	14	2.1
18240+2326	CRL2155	C	1000	1.5	12	1.8
18398-0220	IRC+00365, CRL2233	C	960	2.2	8	1.1
19175-0807	IRC-10502, CRL2368	C	890	1.0	∼12	∼1.6
20570+2714	CRL2686	C	1100	1.0	∼4	∼0.6
—	CRL2688, Egg Nebula	PPN	(750)	(4.1)	11	1.2
—	NGC7027	PN	(940)	(6.3)	—	—
23166+1655	CRL3068	C	1000	3.4	15	2.2
23320+4316	IRC+40540, CRL3116, LP And	C	740	1.0	14	1.6

of high-mass loss AGB stars, with $\dot{M} > 2 \times 10^{-6}$ $M_\odot$ yr^{-1}. This list is thought to be complete for AGB stars out to ~ 1 kpc of the Sun, within the northern hemisphere limits of the TMSS (δ = –33° to +82°). The total number of carbon stars found was 29, of which 13 have mass-loss rates $\geq 10^{-5}$ $M_\odot$ yr^{-1}. These highest mass-loss objects supply $\sim 80\%$ of the total mass-loss in the JK carbon star list, so to limit the observing time required, this subset of 13 stars was chosen to be our source sample. The sample includes three sources that are not strictly AGB stars – CRL915 and NGC7027 are planetary nebulae, while CRL2688 is a protoplanetary nebula.

2. Observations

The carbon stars were observed in carbon monoxide emission in May 1995, using the James Clerk Maxwell Telescope, located on Mauna Kea, Hawaii. The J=2–1 rotational lines were observed, for which the rest frequencies are 230.5380 GHz (^{12}CO, or CO for brevity) and 220.3987 GHz (^{13}CO). At these frequencies, double-sideband system temperatures ranged from 300–500 K using the RxA2 receiver (Davies et al. 1992). Integration times were 3–15 minutes for CO, and 10–35 minutes for ^{13}CO. The observations were made by switching the secondary mirror at 1 Hz, over 2′ in azimuth, which resulted in very flat baselines. The spectra were recorded using a digital auto-correlation spectrometer (DAS), at a spectral resolution of 0.38 MHz, but the data have been regridded here to uniform 1.0 km s^{-1} velocity bins.

The source positions were taken from the catalogue of Loup et al. (1993), except for CRL5254 and IRC+00365, where the positions previously adopted at the JCMT are offset in R.A.-Dec. by (–4″,–8″) and (+1″,–3″), respectively. To establish the exact CO peak, we made five point maps at 10.5″ spacing (half the 21″ FWHM beam size), which also enabled us to estimate the sizes of the circumstellar envelopes (Table 1). The antenna temperatures at the offset positions were modelled by integrating contributions over the beam, assuming gaussian source and beam profiles, and varying the source radius to match the obervations.

For four stars (CRL2135, CRL2155, IRC+00365 and IRC+40540), the catalogued CO positions were corrected by 4–6″, but since we could not point using ^{13}CO, these spectra are at the nominal positions. Corrections for these offsets have been made in the ^{13}CO intensities, and included in the isotope ratio calculations. The gaussian model above was used to find the intensity corrections, which were typically an increase of 10 ($\pm$ 5)% in peak antenna temperature. The error estimate arises from the uncertainties in the fitted source sizes. Finally, for two other stars, IRC-10502 and CRL2686, the position of the CO peak was uncertain, and the nominal positions were used for both lines.

The spectra are presented on the T_A^* antenna temperature scale, corrected for atmopheric opacity. These can be converted to main-beam antenna temperatures T_{mb} by dividing by an efficiency factor of $\eta_{mb} = 0.68 \pm 0.01$, measured on Mars. Calibration measurements (using hot, cold and sky loads) were made before observing each source, to ensure the accuracy of the T_A^* values, and for most of the run, the atmospheric opacity was low (0.05–0.10 at zenith at 230 GHz). Pointing checks were made before observing each source, using the stars themselves for the CO data, and nearby bright continuum sources for the ^{13}CO lines. From the latter data, the average pointing correction was 2″.

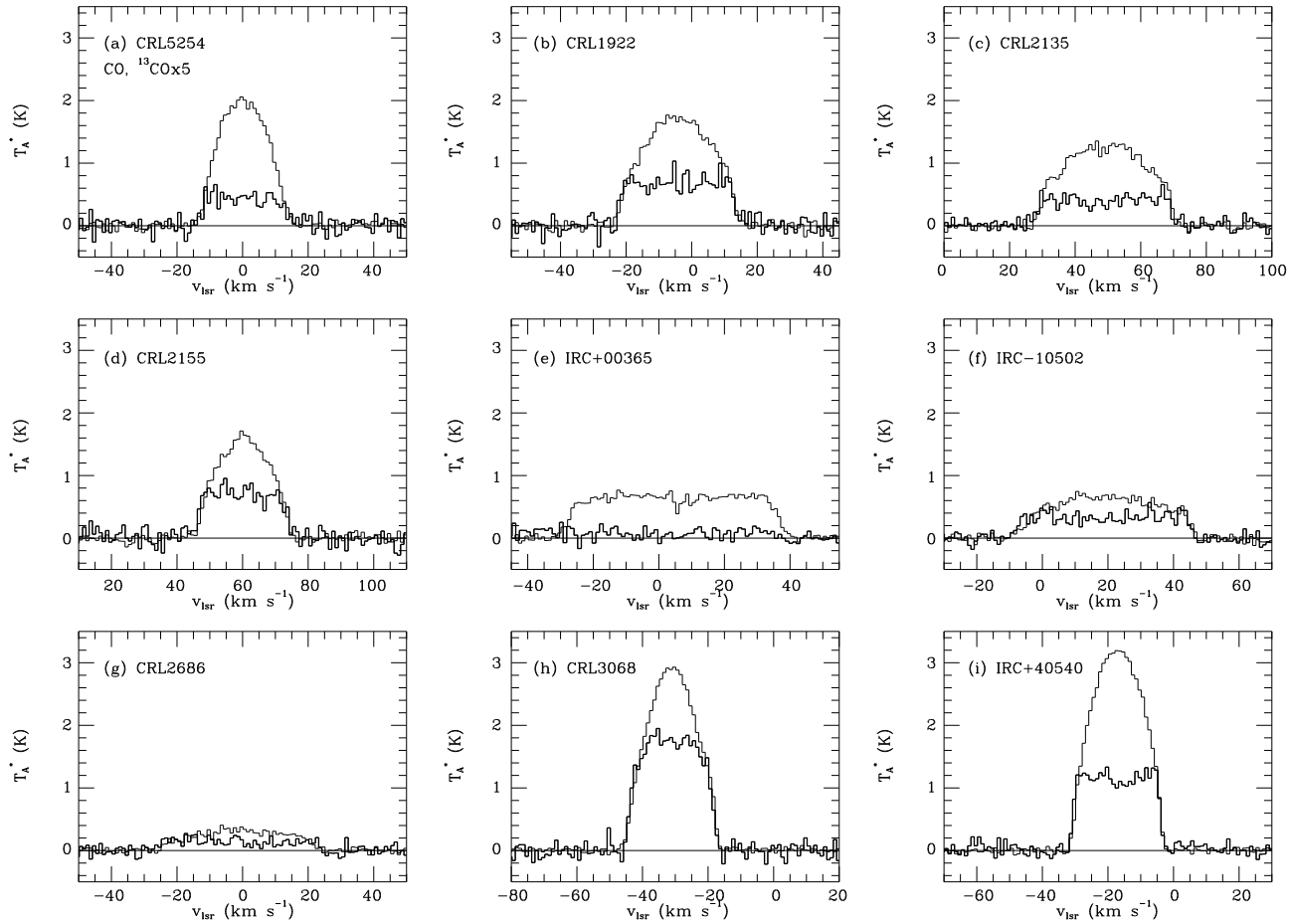

Fig. 1a–i. CO and ^{13}CO J=2–1 spectra of the 9 carbon stars observed in May 1995. The ^{13}CO spectra (thick lines) are multiplied by a factor of 5 in T_A^*.

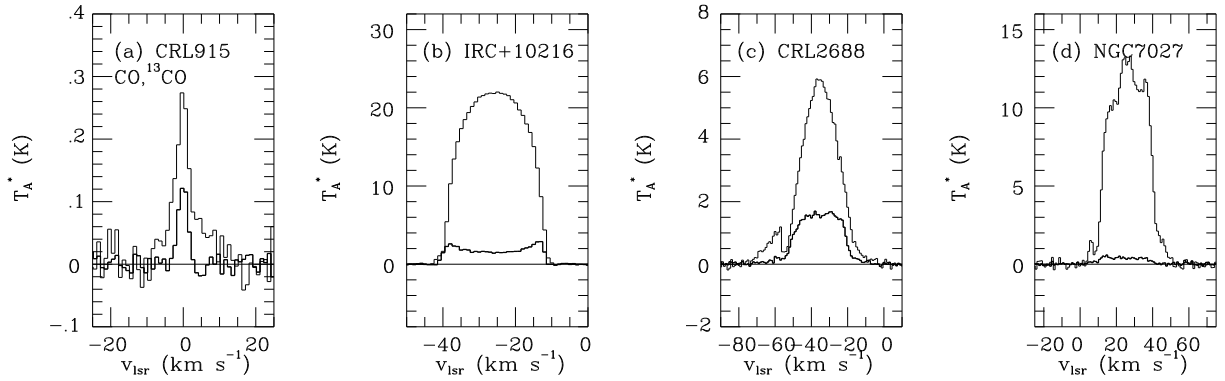

Fig. 2a–d. CO and ^{13}CO J=2–1 spectra of the planetary nebula CRL915 (May 1995 observations), and of the carbon star IRC+10216, the proto-planetary nebula CRL2688, and the planetary nebula NGC7027 (from the JCMT spectral standards and archive databases). Within each plot, the ^{13}CO spectrum (thick line) is shown on the same scale as CO.

The calibration uncertainty in the $^{12}CO/^{13}CO$ ratios is estimated at $\pm$ 5%, or less. This value is based on frequent observations of IRC+10216, which is a JCMT 'spectral standard'. We have searched the standards database to find CO and ^{13}CO J=2–1 spectra made within 1 month of each other (to avoid any problems with possible variability in the molecular emission, over the star's 635 day period). The $^{12}CO/^{13}CO$ integrated-T_A^* ratio for 1994/1995 was 8.6 ± 0.4, which is a $\pm$ 5% range in the relative intensities. The absolute intensity calibration is accurate to about $\pm$ 10% (from the CO data over the same period), with the somewhat larger range reflecting longer-term effects.

3. Results

The properties of the star sample are listed in Table 1, and the observational results are given in Table 2. During the May 1995 run we observed 10 of the stars in the source sample. Spectra of IRC+10216 and CRL2688 were taken from the JCMT standards database, with observations made in March 1995 and October 1994 respectively. Earlier spectra (August/September 1993) of NGC7027 were taken from the JCMT data archive. The spectra for these 13 stars are shown in Figs. 1 and 2.

We also obtained some limited data on the stars' dust emission in the (sub)millimetre regime (Table 3), complementing that of Groenewegen et al. (1993), who previously used the JCMT to observe five of the stars in our sample. Our new data shows comparable flux densities to the Groenewegen et al. results, consistent with stars of similar mass-loss rates and gas-to-dust ratios.

3.1. $^{12}CO/^{13}CO$ *intensity ratios*

The carbon isotope ratios can be initially estimated using the antenna temperature ratios at the line centre, where the optical depth is least. This emission arises in the parts of the envelope close to the plane of the sky, where the line-of-sight velocity in an expanding envelope has the highest gradient, so there is least material contributing to each channel in the spectrum. The T_A^* values for CO and ^{13}CO J=2–1 have been measured over the central 10% of the line profile (5% or 20% in a few cases of steep line profiles or low signal-to-noise), and are listed in Table 2. Corrections for the offsets in ^{13}CO pointing are included where appropriate. The intensity ratios of $T_A^*(^{12}CO)/T_A^*(^{13}CO)$ are also given; these will underestimate $^{12}C/^{13}C$ because the ^{12}CO lines have moderate optical depths (see below), but some general points can be deduced.

The AGB results show, firstly, that there are no very *low* $^{12}CO/^{13}CO$ values, near the minimum of 3.4 attainable in CNO processing. The lowest observed $^{12}CO/^{13}CO$ value for the AGB stars is 8. It has been suggested by Jura et al. (1988) that very ^{13}C-rich carbon stars could have an important effect in changing the local $^{12}C/^{13}C$ ratio in the ISM. They found that about 15% of carbon stars within 600 pc of the Sun were very ^{13}C-rich, with $^{12}C/^{13}C \approx 3$–4 (Lambert et al. 1986), but it was noted that these all have low $\dot{M}$, of a few 10^{-7} $M_\odot$ yr^{-1}. Since none of the high mass-loss stars observed here, which dominate mass return, have very low $^{12}CO/^{13}CO$ values, the evolution of this isotope ratio in the ISM will be less rapid.

Table 2 shows that the $^{12}CO/^{13}CO$ intensity ratios in the sample are fairly uniform. For the 10 AGB stars, the mean ratio is 17 ± 11 (1 σ), but the scatter is dominated by the high value for IRC+00365. (This CO profile is noticeably more flat-topped than the average, and presumably the larger expansion velocity in this source reduces the CO optical depths, increasing the intensity ratio.) Excluding this value, the $^{12}CO/^{13}CO$ intensity ratios lie in the range 13 ± 4, and are thus rather uniform. An exception is the proto-planetary nebula CRL2688, where the CO opacity is high, and thus the T_A^* ratio is only 3.7, much less than the isotope ratio (see Kahane et al. 1992, hereafter K92). This explanation presumably also applies to the planetary nebula CRL915 (the Red Rectangle), since the $^{12}CO/^{13}CO$ intensity ratio increases away from the line centre (Fig. 2). Using only the line wings, seen in CO emission between $|v_{lsr}| = 2$ and 9 km s^{-1}, the integrated intensities give a 1 sigma limit of $^{12}CO/^{13}CO \geq 12.5$.

3.2. Line profiles

Table 2 also lists the centroid velocity of each line, v_0, and estimates of the envelope expansion velocity, v_e, from the zero-emission points in the profiles. Comparing CO and ^{13}CO results, the centroids agree within 0.3 km s^{-1} generally (but 4 km s^{-1} for the weak-line sources IRC+00365 and CRL2686 and the PN NGC7027), and the expansion velocities typically differ by only 1.5 km s^{-1}. These by-eye estimates of v_e therefore appear to be consistent, and they also agree with previous estimates of v_e as summarised by Loup et al. (1993), within $\sim$ 1 km s^{-1}.

An alternative approach to finding the line parameters is to use a line-fitting procedure. We used the expression of Olofsson et al. (1993)

$$T(v) \;=\; T(v_0)\left[1-(v-v_0)^2/v_e^2\right]^{\gamma/2} \qquad (1)$$

where γ is a shape parameter. The values found for γ are listed in Table 2; these are the best fit results, with average reduced χ^2 for the Fig. 1 sources of 1.3 for CO and 0.9 for ^{13}CO. Other fits were found, within a probability limit of $\geq$ 10% in χ-squared tests, and these γ values typically varied by $\pm$ 0.9. (The fits of the CO lines in CRL2135, IRC+00365 and CRL3068, and ^{13}CO in IRC+40540, had somewhat larger reduced χ^2 of 1.7–2.8, below the 10% probability limit, and no γ ranges were found; this was also the case for IRC+10216 where the high data quality exceeds the limitations of the simple profile formula.)

These line fits are useful because the value of γ is an indicator of optical depth, with values ≈ 2 corresponding to parabolic lines (optically thick unresolved envelopes), and values ≈ 0 found for rectangular lines (optically thin unresolved emission). The best-fit results gave average values of γ of 1.5 ± 0.7 for CO, and 0.4 ± 0.3 for ^{13}CO, where the errors are the 1 σ spread. These results confirm that CO has a non-negligible optical depth, and thus the intensity ratios *underestimate* the true isotopic ratios; these are determined in the next section.

Table 2. Parameters of the CO and ^{13}CO J=2–1 lines. For each star, the first line refers to CO, and the second to ^{13}CO. The v_0 and v_e values are the centroid and expansion velocities respectively, γ is the shape parameter from Eq. (1), and T_A^* values are for the central $\approx 10\%$ of the profile, with uncertainties of the standard error over this velocity range. For CRL2135, CRL2155, IRC+00365 and IRC+40540, the ^{13}CO data and the ^{12}CO/^{13}CO ratios include corrections for ^{13}CO pointing offsets, described in the text. The ^{13}CO results are therefore about 10% brighter than direct measurements from the spectra in Fig. 1. The errors in the T_A^*-ratios include the effects of noise in the T_A^* values, the uncertainties in the ^{13}CO correction (where appropriate), and an estimated $\pm$ 5% calibration accuracy, added together in quadrature.

star	v_0 (km s^{-1})	v_e (km s^{-1})	γ	$\int T_A^* dv$ (K km s^{-1})	T_A^* (K)	T_A^* ratio, ^{12}CO/^{13}CO
CRL915	+0.2	9	—	1.80	0.26 ± 0.02	2.2 ± 0.3
	–0.1	3	—	0.41	0.117 ± 0.011	
CRL5254	+0.2	16	2.6	37.6	2.02 ± 0.02	22 ± 1
	0.0	17	0.6	2.41	0.092 ± 0.003	
IRC+10216	–25.7	16	0.9	496.3	21.89 ± 0.05	15 ± 1
	–25.7	15	–0.4	54.3	1.47 ± 0.03	
CRL1922	–4.1	21	1.9	46.4	1.71 ± 0.02	12 ± 1
	–4.1	20	0.5	4.97	0.141 ± 0.012	
CRL2135	+49.5	23	1.3	41.2	1.24 ± 0.04	14 ± 2
	+49.9	23	0.4	4.07	0.087 ± 0.008	
CRL2155	+60.3	17	1.7	32.3	1.64 ± 0.03	10 ± 1
	+59.3	17	0.7	4.37	0.162 ± 0.008	
IRC+00365	+4.1	37	0.3	41.5	0.64 ± 0.03	49 ± 17
	–0.3	37	0.3	1.22	0.013 ± 0.004	
IRC-10502	+19.5	28	1.1	28.3	0.66 ± 0.02	11 ± 1
	+19.6	29	0.1	3.56	0.059 ± 0.004	
CRL2686	–0.4	26	1.2	11.9	0.33 ± 0.02	11 ± 2
	–3.9	26	0.5	1.40	0.029 ± 0.004	
CRL2688	–35.7	31	—	151.7	5.89 ± 0.02	3.7 ± 0.2
	–35.6	33	—	49.6	1.58 ± 0.02	
NGC7027	+26.6	23	—	335.8	12.93 ± 0.09	31 ± 3
	+22.8	18	—	12.3	0.419 ± 0.041	
CRL3068	–31.0	16	2.4	55.4	2.90 ± 0.01	8 ± 1
	–31.3	14	0.9	8.28	0.346 ± 0.008	
IRC+40540	–17.0	14	1.6	63.7	3.18 ± 0.01	14 ± 1
	–17.4	15	0.3	6.67	0.229 ± 0.007	

Table 3. Continuum data for four of the stars in our sample – see also Groenewegen et al. (1993), who observed five more of the stars, also using the JCMT. Flux densities and 1 σ errors are given for wavelengths of 450, 800 and 1100 μm, with beam half-power diameters of 8″, 14″ and 19″, respectively.

star	S(450)	S(800) (mJy/beam)	S(1100)
CRL915	1460 ± 250	629 ± 37	175 ± 16
CRL5254	—	97 ± 14	70 ± 11
CRL2155	—	(129 ± 119)	132 ± 28
CRL2686	—	—	(-7 ± 19)

Table 4. LVG model results for the ABG stars.

star	τ(CO)	T_{mb}(model) /T_{mb}(obs)	^{12}CO/^{13}CO abundance
CRL5254	1.4–3.1	0.65	36
IRC+10216	1.4–2.4	0.86	32
CRL1922	1.3–2.8	0.95	20
CRL2135	0.4–1.7	0.54	17
CRL2155	1.4–3.0	0.91	17
IRC+00365	0.9–1.3	0.95	$\sim$57
IRC-10502	0.8–1.2	0.66	12
CRL2686	1.0–1.3	0.69	14
CRL3068	4.0–5.5	0.92	25
IRC+40540	1.3–3.1	0.74	24

We also note that a range of fits to the centroid T_A^* was generally possible, for different shape parameters. Since the direct estimates of T_A^* have smaller errors, they are used for the isotopic ratio calculations. The value of γ is not well constrained, i.e. a moderate change does not greatly affect the line profile, and a negative γ (profile with a central dip) is in fact possible for some of the ^{13}CO lines. This could indicate envelopes that are spatially resolved (Olofsson et al. 1993), but is more likely to arise because low signal-to-noise ratios allow a wide range of fits, for these particular stars (CRL5254, IRC+00365, IRC-10502 and CRL2686).

3.3. LVG modelling

Since the CO emission is found to be optically thick, radiative transfer modelling is required to find the isotope ratios. Models for expanding circumstellar envelopes are generally based on the assumption of large velocity gradients (LVG), where only one region along the line of sight contributes emission at a particular velocity. Detailed models have been developed to reproduce the observed line profiles from AGB stars (see e.g. Kahane & Jura 1994). However, since we are interested in the $^{12}C/^{13}C$ ratios, we use a simpler LVG model to reproduce only the ratio of CO and ^{13}CO intensities at the line centre.

The radiative and collisional rates for CO are used to find the equilibrium level populations up to J=10. For high mass-loss rates, the envelope is opaque to IR radiation, so IR pumping of the rotational levels has little effect (Kastner 1992), and is omitted in our model. The model output is the antenna temperature T_R (for perfect coupling to the telescope beam), as a function of molecule abundance, velocity gradient, gas kinetic temperature and H_2 volume density. The values of T_R are found for radial zones in the envelope which contribute to $T(v_0)$, and these values are then corrected for beam coupling, and summed to give the expected T_{mb} for the CO line. To find the isotopic ratio, the ^{13}CO abundance was adjusted, relative to that of CO, until the $T_{mb}(^{13}CO)$ values gave the observed $^{12}CO/^{13}CO$ intensity ratio.

Typically five radial zones were used, extending from $r \approx 1''$ out to twice the half-intensity radius (Table 1). Gas densities for each zone were calculated assuming constant mass-loss rates (from JK), and kinetic temperatures $T_{kin}(r)$ were taken from Fig. 1 of Kastner (1992), for a mass-loss of 2×10^{-5} $M_\odot$ yr^{-1}. In fact, the JK values of $\dot{M}$ for our AGB sample are $(1-3)\times 10^{-5}$ $M_\odot$ yr^{-1}, but for simplicity we adopted a single set of kinetic temperatures (the estimated temperature variations affect the isotope ratios by only $\sim 15\%$). The CO/H_2 abundance was taken to be 10^{-3} (Loup et al. 1993). Finally, the radiative decay rates and the telescope beamsizes are slightly different for the CO and ^{13}CO lines, which have a 5% frequency difference, and these effects are included in the modelling.

The isotopic ratios found in the LVG model are listed in Table 4; no modelling was done for the (proto)planetary nebulae, since radial symmetry of the envelope cannot be assumed. The $^{12}CO/^{13}CO$ values for the 10 AGB stars range from 12 to $\sim$57, and are, on average, a factor of 1.65 higher than the intensity ratios. The isotope ratio results agree reasonably well with previous estimates; for example, in IRC+10216 K92 find $^{12}C/^{13}C$ of 44 ± 3 from optically thin lines, and our isotope ratio is about 25% lower.

The CO optical depths found in the modelling are typically about 1–3 (Table 4), and these moderate optical depths are consistent with the flattened paraboloid line shapes. As expected, higher optical depths were found for higher γ values: for stars with an average $\tau(\mathrm{CO}) \geq 2$, the mean γ is 2.0, compared to 1.0 for $\tau(\mathrm{CO}) < 2$ (see Tables 2 and 4).

We note that the LVG model systematically *under*estimates $T_{mb}(\mathrm{CO})$, by an average factor of 0.79 ± 0.14 for the AGB stars (Table 4). This could be explained, for example, by slightly too low mass-loss rates derived by JK, or the presence of some low-level emission around the stars (as found for IRC+10216, see Williams & White 1992 and Huggins et al. 1988). The effects of uncertainties in the mass-loss rates is discussed further below.

4. Discussion

For the 10 high mass-loss AGB stars, we find an average $^{12}CO/^{13}CO$ abundance ratio of 25 ± 13 (1 σ scatter). These isotope ratios are mostly similar, with a range of only 12–36 for 9/10 of the stars, plus a higher, but rather uncertain, value of $\sim$ 57 for IRC+00365. One somewhat lower ratio of ~ 9 has been found previously, in the southern hemisphere high mass-loss carbon star IRAS15194-5115 (Nyman et al. 1993). The isotope range in these sources is therefore $\sim$ 9–57, which is comparable to an earlier study made by Wannier & Sahai (1987). Their CO J=2–1 observations included 7 carbon stars with mass-loss rates $\sim 10^{-5}$ $M_\odot$ yr^{-1}, and the range of $^{12}C/^{13}C$ ratios found was $\approx$ 14–53.

For O-rich high mass-loss AGBs, the carbon isotope ratios tend to be lower than those measured here. Few ^{13}CO observations have been made of the high mass-loss O-stars, but 3 of the 9 $\dot{M} > 10^{-5}$ stars from JK have been detected. For IRC+10011, IRC+20326 and IRC+40004, $T_{CO}/T_{^{13}CO}$ ratios are 6, $\geq$ 9 and 9 respectively (Sopka et al. 1989; Knapp & Chang 1985; Knapp & Morris 1985). If we assume a CO optical depth of ~ 1, the mean isotope ratio is ~ 12. (The optical depth is uncertain, but should be ≥ 1 based on the line shapes, while less than for the carbon stars as the CO abundance is lower). Thus ^{13}C is generally more abundant in the O-rich AGBs than in the carbon stars.

The mean $^{12}CO/^{13}CO$ ratios should accurately measure the mean $^{12}C/^{13}C$ abundance ratios, since although isotopic fractionation can enhance ^{13}CO, and greater self-shielding can enhance ^{12}CO, a study by Mamon et al. (1988) has shown that these effects tend to cancel out in circumstellar envelopes. In the Mamon et al. $\dot{M} = 10^{-5}$ $M_\odot$ yr^{-1} model, the CO abundance is increased relative to ^{13}CO at r of a few 10^{16} cm, but only by $\leq 10\%$. At large radii the $^{12}CO/^{13}CO$ abundance ratio drops below $^{12}C/^{13}C$, but little emission is produced from this region. Thus the CO-based isotope ratios should be accurate to better than 10%.

4.1. Evolution of $^{12}C/^{13}C$ in the ISM

To find the effect of the ejecta from high mass-loss stars on the ISM, we use the formula of K92:

$$x(t) \;=\; x_* + (x_\odot - x_*)e^{-t/\tau} \qquad (2)$$

where x is the ISM abundance relative to H_2 at time t; x_* is the average abundance for the stars, weighted by their mass-loss rates; $x_\odot$ is the solar system abundance; and τ is the characteristic time for ejecta to replace the local matter, i.e. the ratio of Σ, the local ISM surface density, to $\dot{M}$ per square pc, summed for the AGB stars.

The value of τ is 4.3×10^{10} years, for $\Sigma = 13 \pm 2$ $M_\odot$ pc^{-2} (Kulkarni & Heiles 1987; Scoville & Sanders 1987), and

a summed AGB mass-loss rate of 3.0×10^{-10} $M_\odot$ pc^{-2} yr^{-1} (JK). To find $x(t)$, we simplify Eq. (2) by redefining x as the abundance of ^{13}C relative to ^{12}C, thus assuming a cosmic $^{12}C/H$ ratio in the stellar envelopes. Then $x_\odot = 0.011$ (89^{-1}), and x_* is calculated from the mass-loss rates in Table 1 and $^{13}C/^{12}C$ ratios derived from Table 4. We also use $^{13}C/^{12}C$ values for CRL2688 and NGC7027 from K92, and for the southern carbon star IRAS15194-5115 from Nyman et al. (1993).

If only carbon-rich sources are included, which have half the total mass-loss (JK), then $x_* = 0.049 \pm 0.011$. The error comes from considering the range of values if the sources with uncertain $\dot{M}$, such as the PN, are included or not. The $^{12}C/^{13}C$ ratio now, 4.6 Gyr after the formation of the Sun, is then 77 $\pm$ 3. If we include also oxygen-rich stars (with a similar total mass-loss but only 20–50% of the CO/H_2 abundance compared to carbon stars), the estimated x_* is 0.040 ± 0.009, and the current $^{12}C/^{13}C$ ratio is 72 ± 5.

The major uncertainty in this calculation is in the summed mass-loss rate from the stars. The individual $\dot{M}$ from JK are probably uncertain by factors ~ 2, which is the typical discrepancy between the JK values (based on an assumed constant luminosity) and those derived from individual IR luminosities (Claussen et al. 1987), or found from modelling CO line profiles (see Loup et al. 1993 for a summary of such models). In fact, if the JK $\dot{M}$ values are increased by a factor of about 1.55, we can improve the match of our model to the observations. This change for an 'average star' of our sample increases $\dot{M}$ from 1.6×10^{-5} to 2.5×10^{-5} $M_\odot$ yr^{-1}, and the LVG model then gives the mean observed T_{mb}(CO).

We thus consider that the total mass-loss rate, and hence the characteristic time τ, are likely to be uncertain by factors of about 1.5. Including this uncertainty in τ in the calculation of Eq. (2), the current $^{12}C/^{13}C$ ratio is 72 ± 8 (77 ± 5 if only the C-rich sources are included). Changes in $\dot{M}$ also have a small effect on the stellar isotope ratios, and for example, the increased-$\dot{M}$ 'average star' above has $^{12}C/^{13}$ of 22 (c.f. a mean of 25 from Table 4), which would reduce the predicted ISM value of $^{12}C/^{13}C$ from ≈ 72 to ≈ 69.

These predicted values of the ISM $^{12}C/^{13}C$ ratio agree well with observations. The local average ratio is quite well established at $\approx$ 60–70: for example, a value of 62 ± 4 has been found in four local molecular clouds (Langer & Penzias 1993), and 67 ± 2 in diffuse clouds seen towards three nearby stars (Centurión & Vladilo 1991). Our predicted $^{12}C/^{13}C$ ratio is approximately 72 ± 8, which agrees with the ISM values. These current ratios are reduced by about 20–30% compared with the ratio of 89 which existed 4.6 Gyr ago. We conclude that the ^{13}C-enriched ejecta from the high mass-loss AGB stars can explain the present reduced $^{12}C/^{13}C$ ratio in the local ISM.

5. Conclusions

We have measured the $^{12}CO/^{13}CO$ abundance ratio in the 10 northern hemisphere carbon stars with the highest mass loss rates. The isotope ratios range from 12 to $\sim$ 57, and are higher than for high mass-loss O-rich stars. The AGB ejecta are ^{13}C-rich compared to the local ISM, and can explain the decrease of $^{12}C/^{13}C$ from 89 at the time when the Sun formed to $\approx$ 60–70 now. Our data indicate a predicted ISM ratio now of about 72 ± 8, therefore no additional sources of ^{13}C-rich ejecta are required to match the ISM observations.

Acknowledgements. We wish to thank P.G. Williams for some very useful discussions. The JCMT is operated by The Observatories, on behalf of the Particle Physics and Astronomy Research Council of the United Kingdom, the Netherlands Organisation for Pure Research. and the National Research Council of Canada.

References

Centurión M., Vladilo G., 1991, A&A 251, 245
Claussen M.J., Kleinmann S.G., Joyce R.R., Jura M., 1987, ApJS 65, 385
Davies S.R., Cunningham C.T., Little L.T., Matheson D.N., 1992, Int. J. Infrared Millimeter Waves 13, 647
Groenewegen M.A.T., de Jong T., Baas F., 1993, A&AS 101, 513
Huggins P.J., Olofsson H., Johansson L.E.B., 1988, ApJ 332, 1009
Jura M., 1987 in Interstellar Processes, eds. Hollenbach D.J., Thronson H.A., pub. Reidel, p. 3
Jura M., Kahane C., Omont A., 1988, A&A 201, 80
Jura M., Kleinmann S.G., 1989, ApJ 341, 359 (JK)
Jura M., Kleinmann S.G., 1990, ApJS 73, 769
Kahane C., Cernicharo J., Gómez-González J., Guélin M., 1992, A&A 256, 235 (K92)
Kahane C., Jura M., 1994, A&A 290, 183
Kastner J.H., 1992, ApJ 401, 337
Knapp G.R., Chang K.M., 1985, ApJ 293, 281
Knapp G,R., Morris M., 1985, ApJ 292, 640
Kulkarni S.R., Heiles C., 1987 in Interstellar Processes, eds. Hollenbach D.J., Thronson H.A., pub. Reidel, p. 87
Lambert D.L., Gustafsson B., Eriksson K., Hinkle K.H., 1986, ApJS 62, 373
Langer W.D., Penzias A.A., 1993, ApJ 408, 539
Loup C., Forveille T., Omont A., Paul J.F., 1993, A&AS 99, 291
Mamon G.A., Glassgold A.E., Huggins P.J., 1988, ApJ 328, 797
Neugebauer G., Leighton R.B., 1969, Two Micron Sky Survey, NASA SP-3047
Nyman L.-Å, Olofsson H., Johansson L.E.B., et al., 1993, A&A 269, 377
Olofsson H., Eriksson K., Gustafsson B., Carlström U., 1993, ApJS 87, 267
Prantzos N., Aubert O., Audouze J., 1996, A&A 309, 760
Scoville N.Z., Sanders D.B., 1987 in Interstellar Processes, eds. Hollenbach D.J., Thronson H.A., pub. Reidel, p. 21
Sopka R.J., Olofsson H., Johansson L.E.B., Nguyen-Q-Rieu, Zuckerman B., 1989, A&A 210, 78
Truong-Bach, Morris D., Nguyen-Q-Rieu, 1991, A&A 249, 435
Truong-Bach, Nguyen-Q-Rieu, Morris D., Deguchi S., 1990, A&A 230, 431
Wannier P.G., Sahai R., 1987, ApJ 319, 367
Williams P.G., White G.J., 1992, A&A 266, 365
Wilson T.L., Matteucci F., 1992, A&AR 4, 1
Zuckerman B., Dyck H.M., 1986, ApJ 304, 394

This article was processed by the author using Springer-Verlag LaTeX A&A style file *L-AA* version 3.